Rotor Position Identification in Synchronous Machines by Using the Excitation Machine as a Sensor

Simon Feuersänger, Mario Pacas
Universität Siegen, Germany
simon.feuersaenger@uni-siegen.de, jmpacas@ieee.org

***Abstract*- The control of any AC-machine demands the rotor or a flux position to describe the machine. The use of an encoder to solve this problem is possible but this reduces the total reliability of the drive. Encoderless methods can identify the required position by only evaluating the measured electrical quantities of the machine. Generally, additional test signals need to be injected into the machine in the low speed range to extract the desired information. However, in electrically excited medium voltage synchronous machines (EESM), most of the known encoderless solutions fail in the low speed range. In this paper, a novel approach to track the rotor position in a brushless excited EESM is introduced. As the excitation machine is mounted on the same shaft as the main synchronous machine, this approach focuses on the evaluation of the stator quantities of the excitation machines to identify the rotor position. In particular, the electrical asymmetry caused by the rotating rectifier is used to detect the rotor position without the need of injecting any additional test signals. However, like in the case of operation with an incremental encoder, the initial rotor position must be known to obtain the absolute position.**

***Index Terms* —Sensorless control, permanent magnet machines, AC machines, brushless machines**

I. INTRODUCTION

In inverter fed synchronous drives, the knowledge of either the rotor position or of the angle of a certain flux space phasor is mandatory in order to control the drive. Therefore, in conventional drive systems an encoder is installed at the machine shaft, allowing the description and control of the machine at any possible operating point. However, the use of such a sensible mechanical sensor reduces the total reliability of the whole drive system and consequently, a control scheme without encoder is desired in many applications.

The so-called encoderless control for variable speed AC-drives was intensively investigated in the last decades [1], mainly focusing on induction machines or permanent magnet synchronous machines. However, recently, a lot of effort was also dedicated to the electrically excited synchronous machine (EESM), which is commonly used in high power, medium voltage applications.

Now, plenty of methods for different operating conditions are available [2]. Especially the encoderless control in the low speed range or even in standstill is challenging as the induced stator voltages become nearly zero and cannot be used for the identification procedure. In this speed region, most approaches are based on the injection of additional high frequency test signals in order to estimate the rotor position [3]-[8]. However, this leads to higher losses, vibrations, noise and the reduction of the maximum permissible steady state torque.

The high frequency signal injection in medium voltage EESMs is even more challenging. Here the damper winding of the machine suppresses almost all angular dependent information of the test signal response [9]-[11]. Furthermore, if a brushless excitation system is used to feed the field winding of the machine, the situation becomes even worse. This is due to the overall time constant in the field circuit being extremely high and the methods, which evaluate the response of a signal generated by the excitation system fail [7]-[8], [10].

This paper deals with the encoderless identification of the rotor position of the EESM with brushless excitation. However, the introduced approach differs to all prior approaches as not the synchronous machine itself is analyzed but the excitation machine, which is mounted on the same machine shaft. Thus, the idea is to use the excitation machine as a sensor for the rotor position of the synchronous machine.

II. SYSTEM BEHAVIOR

The description of the brushless excitation system of a synchronous drive is quite complex as it comprises two power electronics converters, which both generate non-sinusoidal currents on the corresponding side of the excitation machine.

First, the behavior of the excitation system is explained in order to ease the understanding of the proposed rotor position identification method.

The principal configuration of the excitation system is shown in Fig. 1. It uses a rotating transformer which is fed by the three phase AC power controller for transmitting the power to the rotor. In general, the thyristor converter shown in Fig. 1 exhibits two more legs, which allows to change the rotation direction of the voltage system at the stator winding of the excitation machine by interchanging

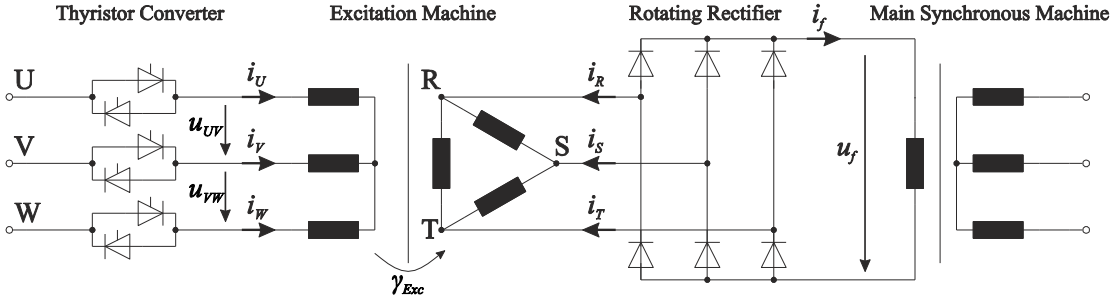

Fig. 1: Conventional setup of a brushless excitation system for a variable speed synchronous drive

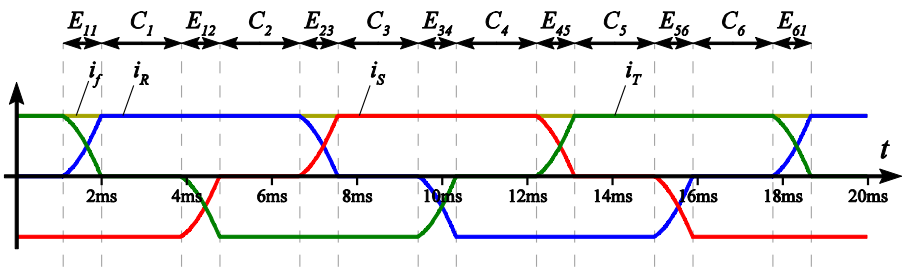

Fig. 2: Rotor currents

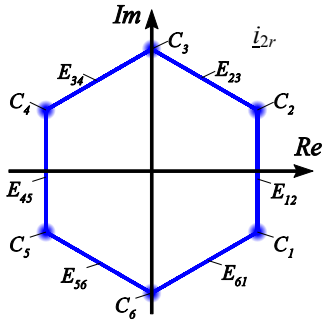

Fig. 3: Trajectory of the space phasor $\underline{i}_{2r}$

the phase sequence. In this way, the operation of the excitation machine with a slip larger than one is guaranteed, regardless of the rotation direction of the main synchronous machine. For the sake of convenience, the additional thyristor legs are not included in the analysis.

On the rotor side of the exciter, a passive diode rectifier in B6-bridge configuration connected to the secondary of the rotating transformer is installed and feeds the field winding of the main synchronous machine. For safety reasons a crowbar, i.e. a thyristor based over voltage protection circuit, is generally included on the rotor side, which is not shown in Fig.1.

By assuming that the B6-rectifier is fed by a symmetrical, sinusoidal voltage system (this is the case, when the control angle of the three phase AC power controller is α=0), the well-known input and output currents as depicted in Fig. 2 are obtained. Due to the usually very large electrical time constant of the field winding of the synchronous machine, the resulting field current i_f becomes nearly constant.

The intervals C_1, C_2, C_3, etc. in Fig. 2 represent the normal states of the rectifier, i.e. the states where exactly one upper and one lower diode of the rectifier is conducting. Consequently, the intervals E_{12}, E_{23}, E_{34}, etc. represent the commutation states in which three diodes are conducting (e.g. one upper and two lower diodes or vice versa). By using the space phasor representation of the three phase rotor currents according to (1) the curve in Fig. 3 is obtained, showing a hexagon, which is the trajectory of the rotor current space phasor $\underline{i}_{2r}$ in the rotor aligned reference frame.

$$\underline{i}_{2r} = \frac{2}{3}\left(i_R + i_S \cdot e^{j\frac{2\pi}{3}} + i_T \cdot e^{j\frac{4\pi}{3}} \right) \qquad (1)$$

In the following, a special notation is used to distinguish the space phasors: The first index shows whether the quantity belongs to the stator winding "1", the rotor winding "2" or is a mutual quantity "*m*". The second index defines the reference frame in which the space phasor is expressed ("*s*" for stator-, "*r*" for rotor fixed reference frame).

In the hexagon in Fig. 3, the corner points C_1, C_2, C_3, etc. refer to the above mentioned normal states of the rectifier whereas the hexagon edges correspond to the commutation states E_{12}, E_{23}, E_{34}, etc. Thus, the trajectory will always remain for a while in the corner points and rapidly pass through the edges to the next corner point.

Now, the overall system behavior including the stator current converter as well as the excitation machine is analyzed. For a better understanding of the interactions between the thyristor converter on the stator side and the rotating rectifier, three states are distinguished:

a) All stator phases of the excitation machine are active

If three thyristors (one per phase) are switched on in a time instant, the grid voltage is directly applied to the stator of the excitation machine. Hence, the excitation machine behaves like a rotating transformer, i.e. the primary voltage is transformed to the secondary side with an additional voltage component caused by the rotation. Like in a conventional transformer, the effective inductance at the rotor side is the sum of the stator and rotor leakage inductances. Therefore, a change of the secondary current also leads to a change of the primary current, without significant changes in the mutual flux.

b) All thyristors are inactive (all stator currents are zero)

In contrast to the first case, the system does not behave like a transformer anymore. Here, the mutual flux is only caused by the rotor currents, leading to a significantly higher effective inductance at the rotor side, i.e. the sum of the mutual inductance and rotor leakage inductance.

c) One phase is inactive

If only two thyristors are conducting at a certain instant (which is a regular state in the thyristor converter), the current in one stator winding becomes zero. Now, the behavior of the system is more complicated as this case is in principle the superposition of the prior cases.

If for instance the stator phase "*U*" is inactive, the current i_U remains zero, which leads to i_V=-i_W. The plot of all possible stator current space phasors $\underline{i}_{1s}$ under this operating condition is shown in Fig. 4. Consequently, if the rotor current changes in that way, that only the imaginary component of the stator current space phasor would be affected, the system behaves like in case a). This is because the changing current in the rotor winding can be compensated by a changing current on the stator side without significant changes in the mutual flux. Thus, the effective inductance at the rotor side is the sum of

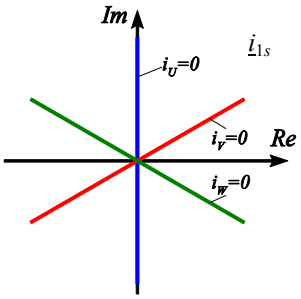

Fig. 4: possible stator current space phasors in state c)

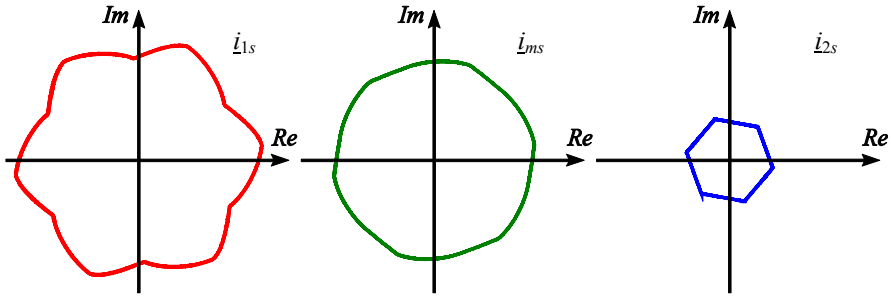

Fig. 5: Trajectory of the space phasors $\underline{i}_{1s}$, $\underline{i}_{ms}$ and $\underline{i}_{2s}$ when maximum voltage is applied to the excitation machine at standstill

the leakage inductances, which leads to a fast changing current on the rotor side.

However, if the rotor current changes in a different way, the real part of the stator current would be affected and the behavior is completely different. In this case, since the real part of the stator current cannot change, a change in the rotor current leads to a change in the mutual flux and the effective inductance at the rotor side is enlarged by the mutual inductance. Therefore, the change in the rotor current is very slow.

Consequently, in this operating point the effective inductance at the rotor side is strongly angular dependent and in general much higher than in state a). If the other phases "*V*" or "*W*" are inactive, the angular dependence of the effective inductance at the rotor side is accordingly different.

If the maximum voltage needs to be applied continuously to the excitation machine, the thyristors are controlled in a way that the system always remains in state a). Fig. 5 shows the space phasors of the stator current $\underline{i}_{1s}$, the magnetizing current $\underline{i}_{ms}$ and the rotor current in the stator fixed reference frame $\underline{i}_{2s}$ obtained at standstill. In this operating point (standstill), the magnetizing current represents the largest portion of the stator current in the given machine. Due to the sinusoidal voltage system applied to the machine, the trajectory of the magnetizing current space phasor $\underline{i}_{ms}$ is nearly a circle. The stator current space phasor $\underline{i}_{1s}$ is the superposition of the magnetizing current and the secondary current in the stator reference frame (2). Because of the hexagonal trajectory of the rotor current, the stator currents become non-sinusoidal.

$$\underline{i}_{1s} = \underline{i}_{ms} - \underline{i}'_{2s} \tag{2}$$

It is self-explanatory that the rotor current space phasor in the stator reference frame $\underline{i}_{2s}$ exhibits the same trajectory like $\underline{i}_{2r}$ in the rotor reference frame (in Fig. 3) but rotated. The rotational angle between both quantities is the electrical rotor position of the excitation machine γ_{Exc}. Hence, if the shaft is rotating, the hexagon in the stator reference frame will rotate with the electrical angular velocity of the shaft.

If the stator voltage of the excitation machine needs to be reduced, the firing pulses of the thyristor converter are changed and the currents in each stator phase become zero for a while (non-conducting mode). Hence, the system switches between states a) and c). Under these conditions, the trajectory of the rotor current space phasor $\underline{i}_{2r}$ differs from the case shown in Fig. 3. Although it follows the same hexagonal trajectory, the rotor space phasor now rests not only in the above explained corner points C_1, C_2, C_3, etc. of the hexagon but also in the here defined intermediate points I_{12}, I_{23}, I_{34}, etc. as shown in Fig. 6. The intermediate points can be explained by observing the stator and rotor currents of the excitation machine in Fig. 7. It is obvious, that the intermediate periods are exactly the intervals in which the thyristor converter is in state c) i.e. where one stator phase is inactive.

As explained above, in this state the effective inductance

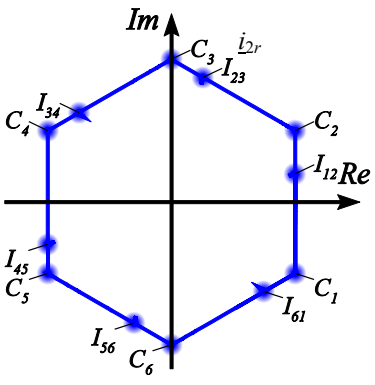

Fig. 6: Trajectory of the space phasor $\underline{i}_{2r}$

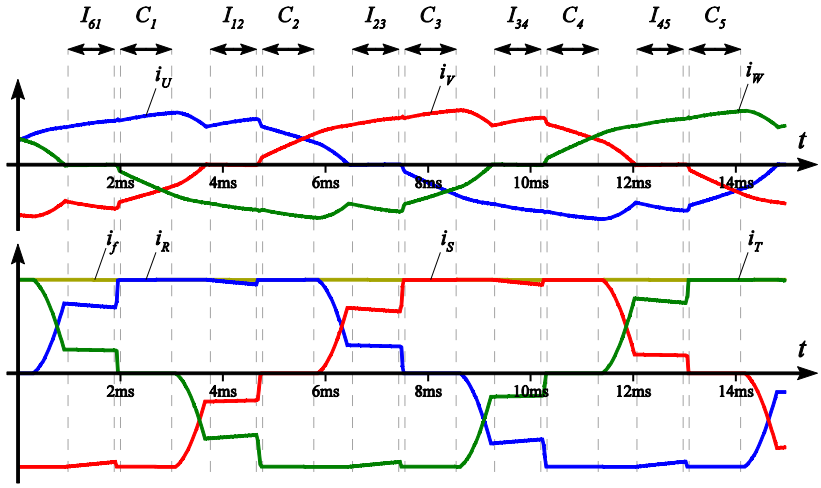

Fig. 7: Stator and rotor currents of the excitation machine

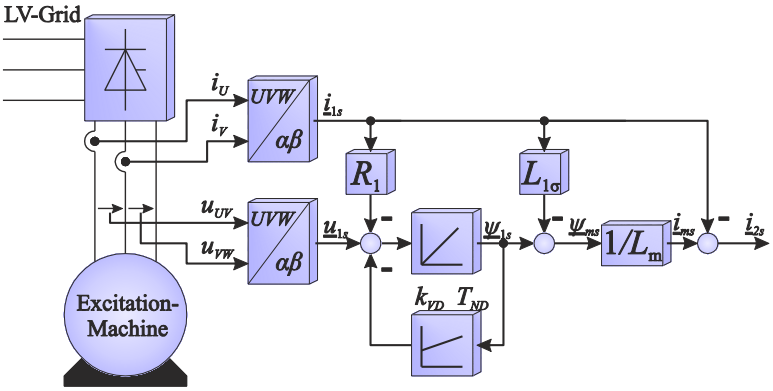

Fig. 8: Machine model to obtain the rotor current space phasor

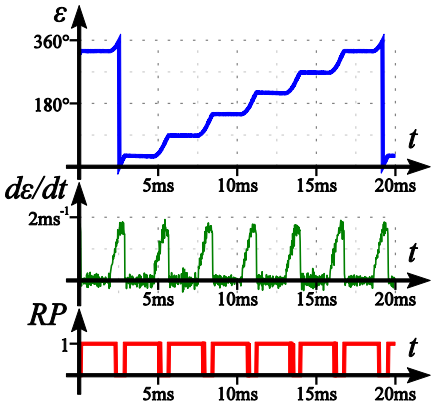

Fig. 9: Rest point identification

at the rotor side is strongly increased as a function of the angular position. In the shown example, the intermediate period lies in the commutation phase of the rotating rectifier and leads to a temporary increase of the effective rotor inductance during this time. Due to the change of the effective rotor inductance, the slope of the rotor current as well as the duration of the commutation are affected. Hence, the temporary increase of inductance forces the commutation to almost stop during the intervals I_{12}, I_{23}, I_{34}, etc., which is the explanation for the additional rest points I_{12}, I_{23}, I_{34}, etc. in the trajectory of the rotor current space phasor.

III. Rotor Position Identification Method

Now the utilization of the above-explained effects for the identification of the rotor position of the main machine is discussed. The main idea is to first calculate the rotor current space phasor in the stator reference frame $\underline{i}_{2s}$. This can be achieved by measuring the accessible stator quantities, i.e. the stator voltages and currents, of the excitation machine and applying the well-known model of the machine as shown in Fig. 8. Hence, in a first step the stator flux space phasor $\underline{\psi}_1$ is obtained by integrating the induced stator voltage. A PI-feedback is used to suppress the drift of the model caused by offsets in the measurement. In a second step, the mutual flux space phasor $\underline{\psi}_m$ and thus the magnetizing current space phasor $\underline{i}_{ms}$ can be computed to finally obtain the desired rotor current space phasor in the stator reference frame $\underline{i}_{2s}$.

$$\Delta\gamma = \gamma_e - \gamma_{Exc} \tag{3}$$

$$\varepsilon = \angle \underline{i}_{2r} \tag{4}$$

Now an estimated rotor angle γ_e is used to calculate the rotor current space phasor in the rotor aligned reference frame $\underline{i}_{2r}$. The idea is, that the angular difference $\Delta\gamma$ which is the difference between the real and estimated rotor position according to (3) can be derived by comparing the obtained trajectory of the identified space phasor $\underline{i}_{2r}$ and the theoretical trajectory shown in Fig. 3 or 6.

The theoretical trajectory of the rotor current space phasor always exhibits its corner points at the angular values 30°, 90°, 150°, 210°, 270° or 330° (Fig. 3 or Fig. 6). Thus, if the trajectory of the estimated rotor current space phasor exhibits its corner points at different angular values, the rotor angle is not correctly estimated. Finally, the angular difference $\Delta\gamma$ can be calculated from the difference between the angular position of an identified and theoretical corner point. This information is used for the correction of the estimated rotor angle. Due to the hexagonal trajectory, this approach leads to a 60° ambiguity in the electrical rotor angle, i.e. the angular difference $\Delta\gamma$ can be a multiple of 60° even under ideal conditions.

The major task is now, to identify the corner points in the identified trajectory. As stated above, the space phasor will always remain for a while in the corner points while rapidly passing through the edges of the hexagon. Thus, the angle ε of the rotor current space phasor $\underline{i}_{2r}$ (4) will not change during the time in which the space phasor rests in one of the corner points. To detect this, the absolute value of the derivative $|d\varepsilon/dt|$ is computed. If this value is below a certain threshold a so called rest point (RP) is detected and the value of the actual rotor current space phasor is stored in $\underline{i}_{RP,i}$. "i" being an increasing number of identified rest points. Fig. 9 shows the angular value ε, its derivative and a signal, which represents that a rest point was detected (signal "*RP*").

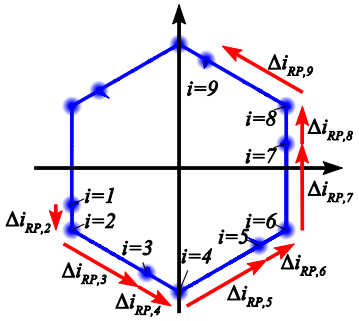

Fig. 10: Difference space phasors

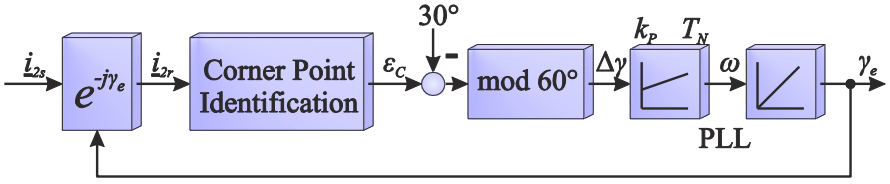

Fig. 11: Estimation of the rotor position with a PLL-structure

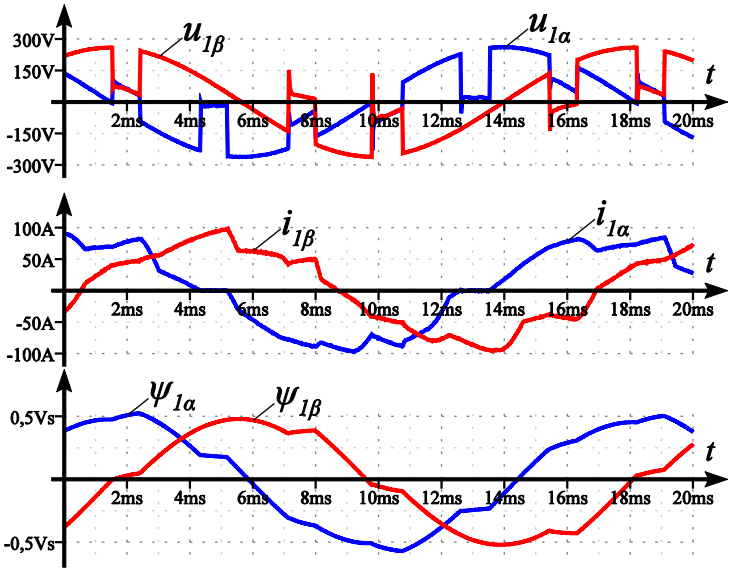

Fig. 12: Stator voltages, -currents, and –fluxes at $180min^{-1}$ (10% n_N)

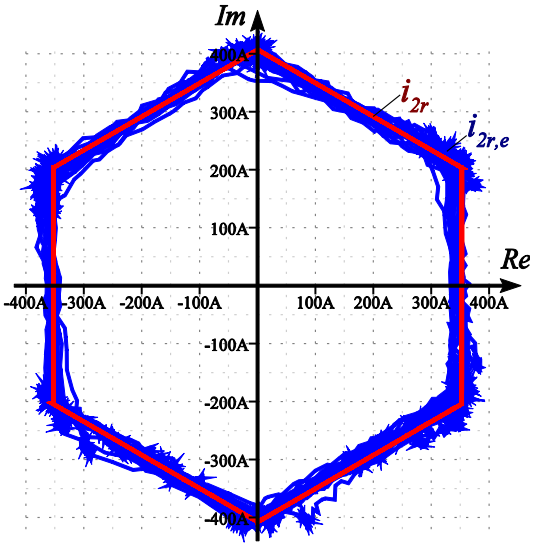

Fig. 13: Estimated ($i_{2r,e}$) and actual (i_{2r}) rotor current space phasor. $180min^{-1}$ (10% n_N)

It is important to mention, that the identified rest point is not necessarily a corner point (C_1 to C_6) of the hexagonal trajectory as also the intermediate points (I_{12}, I_{23}, etc.) shown in Fig. 6 are detected in this way. Thus, the next task is to distinguish whether the identified rest point is a corner point or an intermediate point. For this reason the difference space phasor $\Delta\underline{i}_{RP,i}$ is introduced according to (5) which can be calculated for each identified rest point. $\underline{i}_{RP,i}$ being the value of the identified rotor current space phasor during the identified rest point "i" as stated above.

Consequently, the difference space phasor $\Delta\underline{i}_{RP,i}$ points from the last identified rest point (i-1) to the actual identified rest point (i) as shown in Fig. 10.

$$\Delta\underline{i}_{RP,i} = \underline{i}_{RP,i} - \underline{i}_{RP,i-1} \tag{5}$$

$$\Delta\chi_i = \left|\angle\Delta\underline{i}_{RP,i} - \angle\Delta\underline{i}_{RP,i-1}\right| \tag{6}$$

$$\Delta\gamma = \left(\varepsilon_C - 30°\right) \bmod 60° \tag{7}$$

By observing Fig. 10 it can be concluded, that the direction of two consecutive difference vectors changes if a corner point lies between them. However, the direction will not change at an intermediate point. Hence, in this approach a corner point is identified, if the absolute angular difference between two consecutive difference vectors $\Delta\chi$ exhibits more than 30°. If a corner point is identified, the angular value ε of the rotor current space phasor $\underline{i}_{2r}$ is stored in ε_C and is used for the calculation of the identified angular difference $\Delta\gamma$ (7).

Finally, the rotor position is obtained by a phased locked loop (PLL) structure as shown in Fig. 11, where the corner point identification block includes the strategy mentioned above.

IV. Simulation Results

The encoderless concept was tested by simulation. The machine data was taken from a 10MW brushless excited machine used in a pump. The excitation machine parameters are depicted in table 1.

In order to test the robustness of the approach, the current and voltage signals used for the identification method were numerically reduced to 10bit to simulate the analog to digital converters that are used in the existing control platform. Furthermore, offsets, noise as well as erroneous gains of 1% have been applied in the signal channel to take measurement errors into account.

The obtained stator quantities used for the identification procedure are depicted in Fig. 12 with a machine velocity of $180min^{-1}$. The trajectories of the actual rotor current space phasor i_{2r}, represented in the rotor reference frame, and of the corresponding identified signal $i_{2r,e}$ are shown in Fig. 13.

Fig. 14 shows the performance of the method during a slow speed reversal from +180min^{-1} to -180min^{-1} (±10% of the nominal speed). As already explained, the angular error $\Delta\gamma$ can be a multiple of 60°.

Fig 15 shows the behavior during a faster change in the speed. The actual shaft angle γ_{EXC}, the identified angle γ_e, the angular error $\Delta\gamma$ as well as the normalized actual velocity n/n_N and identified velocity ω_e/ω_N are shown.

Table 1: Excitation machine data

Parameters:

$L_{1\sigma}$	0.76mH	p	4
L_m	4.3mH	f_1	60Hz

Rated data (1800min^{-1}, max. excitation current):

U_1	176V	U_f (DC)	47V
I_1	86A	I_f (DC)	587A

Standstill:

U_1	322V	U_f (DC)	35V
I_1	113A	I_f (DC)	430A

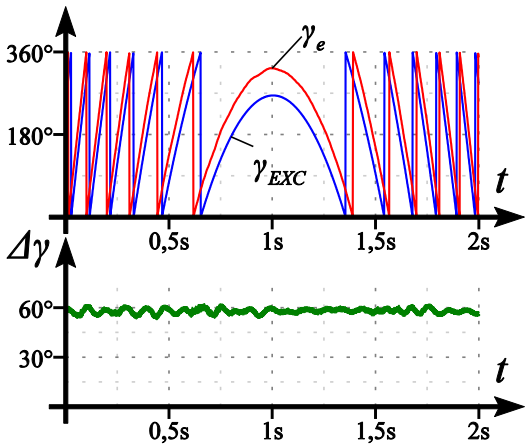

Fig. 14: Slow speed reversal

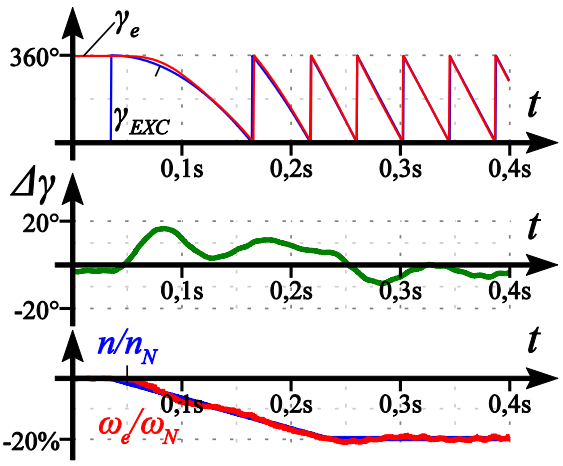

Fig. 15: Rapid change in speed

V. Conclusion

A novel encoderless identification procedure to detect the shaft position in electrically excited synchronous machines with brushless excitation was introduced. In contrast to conventional identification methods, only the signals of the excitation machine are analyzed to extract the information of the rotor position.

The method takes advantage of the hexagonal trajectory of the rotor current space phasor caused by the rotating rectifier to finally track the shaft position. In this way, the electrical rotor position can be identified with 60° ambiguity without any additional signal injection. In order to eliminate the ambiguity in the identified signal, the initial rotor position should be measured as suggested in [10].

A numerical simulation was performed to confirm the proposed method. The results show that the method is especially suitable for the low speed and standstill operation of the drive and allows the tracking of the rotor position even under changing velocities or field current set points.

VI. Outlook

In the future, the proposed method will be tested on a medium voltage synchronous drive in order to confirm the applicability of this method in an industrial environment.

Additionally, the measurement of the line voltages and estimation of the stator voltages instead of directly measuring the stator voltages will be discussed as the possibility for the reduction of the amount of required sensors. Since the line voltages are always measured this would avoid extra hardware.

References

[1] Pacas, M.; "Sensorless Drives in Industrial Applications", Industrial Electronics Magazine, IEEE vol. 5, no. 2, pp.16-23, June 2011

[2] Holtz, J.; "Speed estimation and sensorless control of AC drives", Industrial Electronics, Control and Instrumentation, 1993. Proceedings of the IECON '93., International Conference on, pp.649-654 vol.2, Nov 1993

[3] Linke, M.; Kennel, R.; Holtz, J.: "Sensorless speed and position control of synchronous machines using alternating carrier injection", Electric Machines and Drives Conference, 2003. IEMDC'03. IEEE International, vol.2, pp. 1211- 1217 vol. 2, 1-4 June 2003

[4] Schroedl, M.; "Sensorless control of AC machines at low speed and standstill based on the "INFORM" method", Industry Applications Conference, 1996. 31. IAS Annual Meeting, IAS '96., Conference Record of the 1996 IEEE, vol.1, pp.270-277 vol.1, Oct 1996

[5] Rambetius, A.; Ebersberger, S.; Seilmeier, M.; Piepenbreier, B.: "Carrier signal based sensorless control of electrically excited synchronous machines at standstill and low speed using the rotor winding as a receiver", 15th European Conference on Power Electronics and Applications (EPE), 2013, pp. 1-10, Sept. 2013

[6] Rambetius, A.; Piepenbreier, B.: "Comparison of carrier signal based approaches for sensorless wound rotor synchronous machines", International Symposium on Power Electronics, Electrical Drives, Automation and Motion (SPEEDAM), 2014, pp. 1152-1159, June 2014

[7] Alaküla, M.; "On the Control of Saturated Synchronous Machines", Ph.D. dissertation, Dept. IEA, Lund Institute of Technology, Lund, Sweden, 1993

[8] Uzel, D.; Peroutka, Z.:"Resolver Motivated Sensorless Rotor Position Estimation of Wound Rotor Synchronous Motors", IEEE International Symposium on Industrial Electronics (ISIE), 2013, pp. 1-6, May 2013

[9] Feuersänger, S.; "Drehgeberlose Identifikation der Rotorlage der elektrisch erregten Synchronmaschine in Mittelspannungs-antrieben", Ph.D. dissertation, Universität Siegen, Siegen, Germany, 2015

[10] Feuersänger, S.; Pacas, M., "Initial rotor position detection in synchronous machines using low frequency pulses", IECON 2014 - 40th Annual Conference on, Oct. 2014

[11] Feuersänger, S.; Pacas, M.: "Enhanced estimation of the rotor position of MV-synchronous machines in the low speed range", in Energy Conversion Congress and Exposition (ECCE), 2015 IEEE, pp.4481-4487, 20-24 Sept. 2015